Generation of mega-electron-volt electron beams by an ultrafast intense laser pulse

Xiaofang Wang

Shanghai Institute of Optics and Fine Mechanics, Chinese Academy of Sciences, P.O. Box 800-211, Shanghai 201800, China, and Center for Ultrafast Optical Science, University of Michigan, Ann Arbor, Michigan 48109-2099

Ned Saleh, Mohan Krishnan, Haiwen Wang, Sterling Backus,* Margaret Murnane,* Henry Kapteyn,* and Donald Umstadter

Center for Ultrafast Optical Science, University of Michigan, Ann Arbor, Michigan 48109-2099

Quandong Wang and Baifei Shen

Shanghai Institute of Optics and Fine Mechanics, Chinese Academy of Sciences, P.O. Box 800-211, Shanghai 201800, China

Received April 11, 2002

Mega-electron-volt (MeV) electron emission from the interaction of an ultrafast ($\tau \sim 29$ fs), intense ($>10^{18}$ W/cm^2) laser pulse with underdense plasmas has been studied. A beam of MeV electrons with a divergence angle as small as 1° is observed in the forward direction, which is correlated with relativistic filamentation of the laser pulse in plasmas. A novel net-energy-gain mechanism is proposed for electron acceleration resulting from the relativistic filamentation and beam breakup. These results suggest an approach for generating a beam of femtosecond, MeV electrons at a kilohertz repetition rate with a compact ultrafast intense laser system.

OCIS codes: 320.7120, 270.6620, 350.4990

1. INTRODUCTION

The development of high-intensity lasers has made it possible to study extreme physics on a tabletop. Among the studies, the generation of mega-electron-volt (MeV) electrons by high-intensity laser pulses is of fundamental interest, relevant to relativistic nonlinear optics, laser based accelerators, laser-induced nuclear processes, and the ICF (inertial confinement fusion) fast ignition scheme.[1] An ultrafast, MeV electron beam can also be applied in ultrafast electron diffraction, generation of ultrafast x and γ rays, and as a photocathode electron gun of high brightness.[2–4]

MeV electrons have been observed in a number of high-intensity interaction experiments with 150-fs to 1-ps laser pulses.[5] Compared with a plasma oscillation period $\tau_p = 2\pi(\epsilon_0 m/n_e e^2)^{1/2}$ (where m is the electron mass and n_e is the plasma electron density), the laser pulse durations were long. In the interactions there were at least several plasma oscillation periods in the laser pulse envelope or there was a greater gradient of the laser field in the transverse direction than in the propagation direction of the laser pulse. Though various acceleration mechanisms have been invoked in interpretation of the energetic electrons, such as plasma wave acceleration, ponderomotive laser acceleration, and direct laser acceleration,[5–16] the net energy gain of the accelerated electrons is still a subject of research because of the complexity of the interactions and possible synergetic action of various mechanisms.

With a shorter laser pulse whose pulse width is close to the plasma oscillation period, the interaction physics may change a lot, which will in turn affect the generation of MeV electrons. However, studies of MeV electron generation at shorter pulse durations have been few, owing to the difficulty of producing high-intensity pulses with such short durations. Only recently, with the advent of ultrafast, high-intensity lasers, have there been a few experiments on the generation of MeV electrons.[17–19] Despite these results, further studies are necessary, especially of the interaction physics of such an ultrafast laser pulse with matter and possible new approaches to MeV electron generation. In this paper we present our studies on the MeV electron emission driven by an ultrafast intense laser pulse in a regime in which the laser pulse's longitudinal spatial extent is close to or shorter than both the focal spot size and the plasma oscillation wavelength. A beam of MeV electrons is generated, and the electron emission is discovered to be strongly correlated to relativistic filamentation of the laser pulse in underdense plasmas. A new net-energy-gain mechanism is proposed for interpreting the origin of the MeV electrons through the laser intensity decrease that is due to relativ-

0740-3224/2003/010132-06$15.00

istic filamentation and beam breakup. These results suggest an approach for generating a beam of MeV electrons at a kilohertz (kHz) repetition rate with a compact kHz laser system.[20]

2. EXPERIMENT

The experiments were performed with a tabletop, multiterawatt, ultrafast Ti:sapphire laser system that delivered 29-fs pulses at 810 nm with repetition rate of 10 Hz.[17,21] The intensity contrast was measured as $\sim 10^{-5}$ on the nanosecond scale. High-dynamic-range pulse width measurements (Fig. 1) showed that the laser pulse shape was well approximated by a superposition of two Gaussian temporal profiles, one having $\tau = 28.4$ fs full width at half-maximum (FWHM) and the other having $\tau = 110$ fs FWHM. The laser pulse contained 93% of the laser energy in the range from the pulse peak to ± 38 fs, beyond which there were wings, extending to ± 200 fs, with less than 7% of the laser energy. The wings were due to incomplete compensation by the grating compressor, resulting in an intensity contrast better than 10^{-5} at ± 200 fs. The horizontally linear-polarized, 4-cm-diameter laser beam was focused with an $f/4.5$, 45° off-axis parabolic mirror onto a supersonic gas jet. The vacuum spot size (see Fig. 2) was $r_0 = 8\ \mu$m (radius in $1/e^2$ intensity), containing 50% of the laser energy. For incident laser power $P = 6$ TW, this led to peak intensity $I = 3 \times 10^{18}$ W/cm^2 or $a_0 = 1.2$ (a_0 is the laser strength parameter, given by $8.5 \times 10^{-10} \lambda\ [\mu\text{m}] I^{1/2}\ [\text{W/cm}^2]$). The supersonic gas jet, which forms a 750-μm-diameter, sharp-edged flat-top-profile gas plume, was backed by N_2 or H_2 to produce the required plasma electron density[22] up to 10^{20} cm^{-3}, or $n_e = 0.06 n_c$ (where n_e is the plasma electron density and n_c is the critical density, which for 810 nm equals 1.7×10^{21} cm^{-3}). The plasma density was calibrated with Raman backscatter by a long pulse at low intensity ($\sim 10^{17}$ W/cm^2), and the density fluctuation ranged from $\pm 20\%$ at $n_e = 1 \times 10^{20}$ cm^{-3} to $\pm 40\%$ at $n_e = 6 \times 10^{18}$ cm^{-3}. At lower densities ($\lesssim 10^{18}$ cm^{-3}) deviations from nominal values reached $+100\%$ for a few density data. A barrier-suppression ionization model[23] indicates that a stable ionization stage or plasma electron density is obtained because nitrogen is ionized to helium-like ionization states above a laser intensity of 1.4×10^{16} W/cm^2 and below 1.0×10^{19} W/cm^2. Thus ionization-induced defocusing should not be significant.

Unlike previous long-pulse experiments in which relativistic self-focusing and Raman scattering were usually observed,[24,25] under the present experimental conditions we found that Raman scattering was not significant, and we observed clearly relativistic filamentation, which, when the incident laser power was greater than some value, caused beam breakup by scattering the laser beam out of the vacuum propagation angle. When the incident laser power $P \approx P_c$, where P_c is the power threshold for relativistic self-focusing, relativistic filamentation began to grow; when $P \geqslant 5P_c$, the laser beam's scattering was evident.[17] The observed relativistic filamentation and beam breakup are shown in Fig. 2. The apparent size of these filaments is 4–5 μm (see the image with $n_e = 0.035 n_c$), close to the resolution limit of the imaging

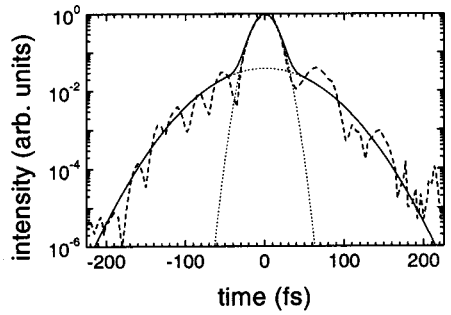

Fig. 1. High-dynamic-range pulse measurement with a frequency-resolved optical gating (FROG) technique. Dashed curve, experimentally measured result; solid line curve, fitted profile, which is the superposition of two separate Gaussian temporal profiles (dotted curves) of 28.4 and 110 fs FWHM.

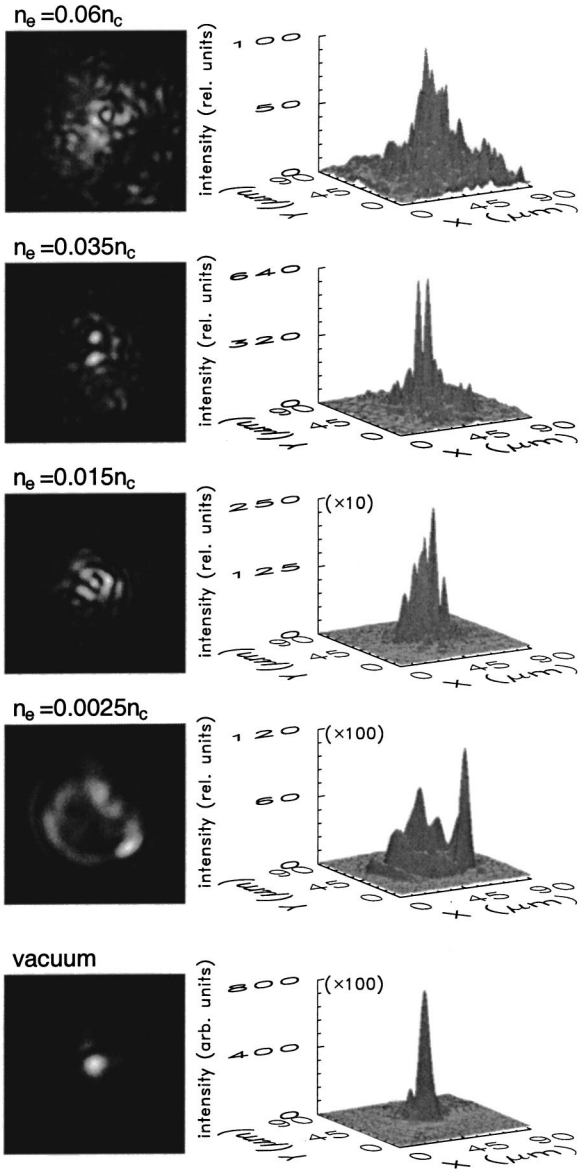

Fig. 2. Microscopic images of the transmitted light as a function of plasma density and the corresponding intensity distributions for an incident laser power of 6 TW. The image labeled vacuum is the laser beam image at the best focal position under vacuum, and the other images correspond to 400 μm beyond the best vacuum focal position.

system that was used in the measurement.[17] Note that the filament size is smaller than the vacuum spot size (9 μm FWHM) of the laser beam.

3. MeV ELECTRON EMISSION

Along with the growth of relativistic filamentation, MeV electrons were observed to be emitted in the forward direction. A plastic scintillator coupled to a photomultiplier tube (S–PMT, which was calibrated with a radioactive source), read out by an oscilloscope, was placed outside the vacuum chamber window of enhanced Mylar foil, to record, in the forward direction, the number of electrons. As is shown in Fig. 3, the S–PMT measurement for the MeV electrons exhibits two features: (i) for $P \approx 6$ TW, the electron signal first appears at $n_e = 0.015n_c$, which corresponds to $\tau/\tau_p = 1.32$, and increases with increasing plasma density. There is no electron signal at lower plasma densities. Note that at this density there was an evident reduction of the transmitted laser light.[17] (ii) For $n_e = 0.06n_c$, the electron signal first appears at laser power $P \approx 2$ TW and increases with increasing laser power. For either density, electrons are generated only when the incident laser power $P \geqslant 5P_c$. These observations indicate a strong correlation between relativistic filamentation and the MeV electron emission.

A scintillator screen (Lanex) imaged by a 16-bit CCD was placed in the forward direction of the laser beam to provide the angular distribution of the electron beam.[25] The Lanex measurement shows that the electrons are emitted as a collimated beam in the forward direction. The full angular spread of the beam is ~15°. However, there is a main beam component of the whole beam, as shown in Fig. 4, that has a divergence angle of only 1° FWHM. In combination with the S–PMT measurement, we estimate that for $n_e = 0.06n_c$ the number of electrons with kinetic energies above 1 MeV is $\sim 10^5$ and that the number of electrons in the main beam component is $\sim 5 \times 10^4$. Note that the number of electrons is smaller than in previous measurements with a longer laser pulse.[14,24,26] Since we have not seen evidence of whole-beam optical guiding, which has previously been found to be correlated with a decrease in the divergence of electron beam,[25] it appears that these electrons in the main beam are generated from other process (discussed below).

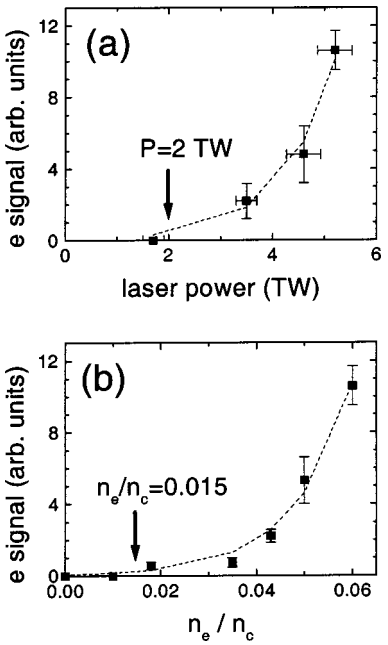

Fig. 3. Measured MeV electron signal (a) as a function of laser power for plasma density $n_e = 0.06n_c$ and (b) as a function of plasma density for laser power $P \approx 6$ TW. The error bars indicate shot-to-shot fluctuations. The numbers and arrows indicate the threshold for observing the MeV electrons. The dashed curves assist the eye.

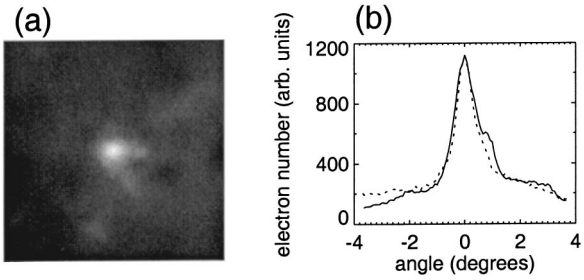

Fig. 4. (a) Lanex image of the main electron beam component and (b) lineouts in the horizontal (solid curve) and vertical (dotted curve) directions through the beam center.

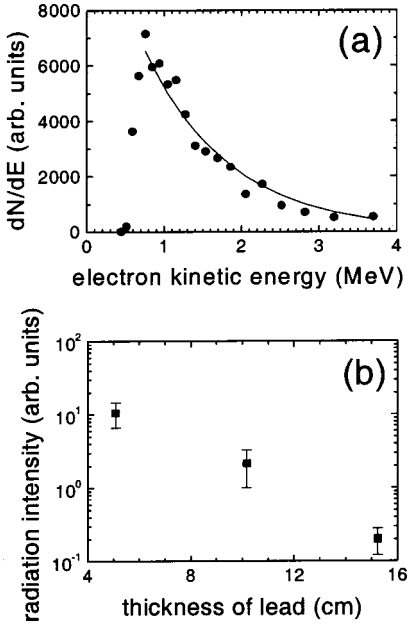

Fig. 5. (a) Measured electron number distribution versus energy (points) and exponential decay fit (solid curve). (b) Measured radiation intensity as a function of lead thickness. Error bars indicate shot-to-shot fluctuations. The incident laser power $P = 6$ TW, and the plasma density $n_e = 0.06n_c$.

The energy spectrum of the electrons, passing through a 2.4° aperture collimator in the direct forward, was measured with a magnetic spectrometer. The result is shown in Fig. 5(a), which is an average of a number of shots with similar laser and plasma conditions. At low electron kinetic energy, the number is underestimated because of the nonlinear dispersion of the spectrometer. It is found that the number of electrons versus energy fits an expo-

nential decay $dN/dE \propto \exp(-E/T_e)$, with temperature $T_e = 1.1$ MeV.

When such electrons impinge upon a material, γ and x radiation will be generated from the bremsstrahlung radiation and secondary scattering processes. Using lead as the material, we measured the generated radiations with an S–PMT placed behind lead bricks, in the forward direction of the electron beam. By changing the thickness of the lead bricks, we found that the radiation could penetrate more than 15 cm of lead. The result is shown in Fig. 5(b).

4. DYNAMICS OF NET ENERGY GAIN DUE TO RELATIVISTIC FILAMENTATION

Besides other net-energy-gain mechanisms of electron acceleration,[5–16] for an ultrafast laser pulse undergoing relativistic filamentation and beam breakup, free electrons accelerated in the laser field could obtain a significant amount of energy by a specific net-energy-gain mechanism that originates from longitudinal ponderomotive laser acceleration.[27] The physics picture is that, when starting from some position along the direction of propagation, the field intensity of an ultrafast, intense laser pulse decreases rapidly; electrons leaving the pulse experience the action of pondermotive deceleration at the descending part of the pulse with lower intensity rather than acceleration at the ascending part of the pulse with high intensity and thus gain net energy from the pulse and move in the forward direction.

In the following we use a test particle model for further analyses. The laser is linearly polarized. Its intensity decrease along the propagation direction that is due to beam breakup is modeled by our introducing an attenuation coefficient, and the normalized vector potential of the laser field is assumed to be[27]

$$\mathbf{a} = a_0 \sin^2\left(\frac{z - Ct}{Ct_0}\right)\sin(\omega t - kz) \times \exp[-\alpha(z - z_0)]\hat{x} \quad (z < z_0,\ \alpha = 0;\ z \geqslant z_0,\ \alpha > 0). \quad (1)$$

a_0 is the laser strength parameter; α is the attenuation coefficient; ω, k, and C are the angular frequency, wave vector, and velocity of the light in vacuum, respectively. The laser pulse has a sine-square temporal profile for its field, and its pulse width $\tau = 1.14t_0$. The vector potential $\mathbf{A}$ is related to $\mathbf{a}$ by $\mathbf{A} \equiv (mC/e)\mathbf{a}$, in which m and e are the electron's mass and elementary charge, separately. The electric field and the magnetic field of the laser pulse are calculated with the Maxwell equations, $\mathbf{E} = -\partial\mathbf{A}/\partial t$ and $\mathbf{B} = \nabla \times \mathbf{A}$. An electron's motion under the laser's electromagnetic field is governed by relativistic motion equations:

$$\frac{d(\gamma m\mathbf{V})}{dt} = (-e)(\mathbf{E} + \mathbf{V} \times B), \quad (2)$$

$$\frac{d(\gamma mC^2)}{dt} = (-e)\mathbf{E} \cdot \mathbf{V}, \quad (3)$$

in which $\mathbf{V}$ is the electron's speed and γ is the relativistic factor, given by $\gamma = 1/(1 - V^2/C^2)^{1/2}$. By inserting $\mathbf{E}$ and $\mathbf{B}$ and solving the two equations numerically, one can obtain the electron's trajectory, momentum, and kinetic energy separately. Suppose that the interaction region z ranges from 0 to 100 μm, in which there exist free electrons that are at rest before the laser pulse arrives. The laser pulse, whose central wavelength is assumed to be 800 nm, propagates with a constant peak intensity along the z axis from the outside into this region, and at the position $z = z_0 = 50$ μm the laser field intensity begins to decrease.

A typical result is shown in Fig. 6, which gives the final velocities of electrons, initially located at different positions along the z axis, after the laser pulse traverses them. The laser pulse has a pulse width of 30 fs FWHM. It turns out that when the intensity of the laser pulse decreases significantly over a short distance, some electrons, being accelerated by the laser field, can gain net energy after the pulse overtakes them. Moreover, it is found from the calculations that these net-energy-gain electrons are emitted directly forward along the direction of the laser pulse's propagation.

Figure 6 also shows that only the electrons initially in a limited region can gain net energy after the laser pulse overtakes them. Outside this region electrons cannot gain net energy. The detailed dynamics is shown in Fig.

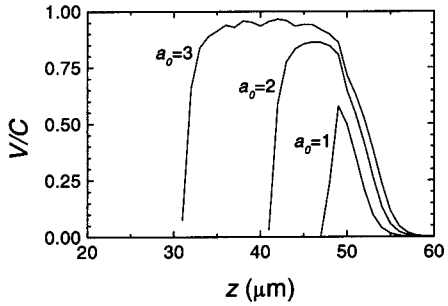

Fig. 6. Final velocities V/C of the electrons, after the laser pulse traverses them, as a function of their initial positions z. The laser pulse propagates along the z axis (from left to right in the plot) and its pulse width is 30 fs in FWHM. The laser's intensity begins to decrease from the position $z = 50$ μm with an attenuation coefficient $\alpha = 0.5$ μm^{-1}. The laser strength parameters are $a_0 = 1, 2, 3$.

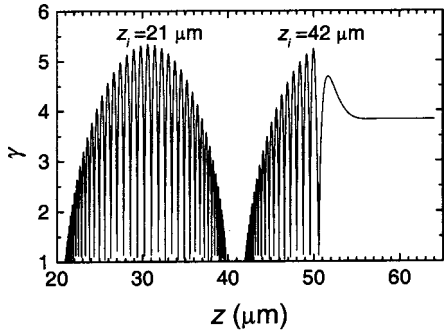

Fig. 7. The relativistic factors γ of two representative electrons as a function of their longitudinal positions z. The two electrons are initially at $z_i = 21$ μm and $z_i = 42$ μm. For the laser pulse, $a_0 = 3$ and the other conditions are the same as described in Fig. 6.

7, which gives a comparison of the relativistic factor, γ, as a function of the longitudinal positions z for two representative electrons, initially located at two positions. One represents electrons that cannot gain net energy after the laser pulse traverses them, the other represents electrons that can. The first electron (without energy gain) experiences the well-known two equal but opposite processes of acceleration and deceleration.[28,29] At the ascending part of the laser pulse, the electron is accelerated and obtains kinetic energy from the laser field. At the descending part of the pulse, it is decelerated and returns an equal amount of the energy to the laser field. Thus the electron obtains zero energy gain after the laser pulse traverses it. The second electron (with energy gain) is accelerated and obtains kinetic energy, like the first one, at the ascending part of the laser pulse. But at the descending-part of the pulse the electron, while moving into the field-intensity-decreasing region, is decelerated by a laser field of lower intensity than in the ascending part because the intensity is decreasing. The net effect is that the electron returns less of the kinetic energy to the laser field during deceleration. As a result, the electron retains an amount of kinetic energy and is emitted forward after the laser pulse traverses it.

As electrons in only a limited region can obtain net energy gain during the acceleration, these electrons, as a pulsed beam, are of a bunch length of the order of femtoseconds (where bunch length is an electron beam's longitudinal spatial extent divided by the velocity of light). In Fig. 6 it is shown that for $a_0 = 3$, i.e., a laser peak intensity corresponding to 2×10^{19} W/cm^2, this limited region corresponds to a bunch length of 90 fs for the electron beam. Experimentally, if free electrons are initially confined in a narrower region, with a thin film target for example, the bunch length of the accelerated electron beam may be shorter.

Further calculations indicate that with the present net-energy-gain mechanism the maximum energy gain of the electrons scales with the laser strength parameter a_0 as ηa_0^2, in which η is larger if the laser pulse is shorter and its intensity decreases faster. For the model calculations ($\alpha = 0.5\ \mu\text{m}^{-1}$) $\eta = 0.43$.

5. DISCUSSIONS AND CONCLUSIONS

Previous theories and simulations have shown that electrons accelerated in a relativistic laser channel or a filament could have high energies and small angular spreads.[15,30,31] For the present experimental studies, since a correlation between MeV electron emissions and relativistic filamentation and beam breakup has been observed, it appears that the MeV electrons are emitted because of beam breakup following the relativistic filamentation. Therefore the net energy gain discussed in Section 4 should contribute to the generation of the MeV electrons. On the other hand, particle-in-cell simulations indicate that under the experimental conditions plasma waves can be excited by the laser pulse before breakup, and thus some electrons may be trapped and further accelerated by a plasma wakefield.[32] However, if the net energy gain discussed above is dominant, then the measured kinetic energy (>3.7 MeV) of the MeV electrons [see Fig. 5(a)] implies that in plasmas the laser beam could be focused to an intensity $a_0 > 4$, as deduced from Section 4.

The present work could be extended to a kHz laser system, for which 0.2 TW/20 fs output has been reported.[33] With a recently implemented technique for generating a near-diffraction-limited beam,[34] a 0.2-TW laser pulse could be focused to 10^{19} W/cm^2, which should be able to generate a beam of femtosecond, 1-MeV electrons directly by means of the net-energy-gain mechanism discussed above. Thus a femtosecond, MeV electron beam could be generated at a kHz repetition rate.

In conclusion, we have observed MeV electron emissions from relativistic filamentation and beam breakup of an ultrafast intense laser pulse. The electrons are emitted as a beam in the forward direction; the divergence of the electron beam is only 1° FWHM. A novel net-energy-gain mechanism from longitudinal ponderomotive laser acceleration has been proposed to explain the origin of the energetic electrons. These results, together with the net-energy-gain mechanism, could be extended to the generation of femtosecond, MeV electron beams at a kilohertz repetition rate with a compact kHz laser system. The generated electron beam may, as a seed, be further accelerated by plasma waves, or be applied either as a femtosecond injector for accelerators or as a beam for the generation of ultrafast radiation sources.

ACKNOWLEDGMENTS

This work was supported by the Outstanding Talents Program of the Chinese Academy of Sciences. The experiment performed at the University of Michigan was supported by the U.S. Department of Energy High-Energy Physics Branch and the U.S. National Science Foundation.

Xiaofang Wang's e-mail address is wangxf @mail.shcnc.ac.cn.

*Present address, JILA and Department of Physics, University of Colorado, Boulder, Colorado 80309-0440.

REFERENCES AND NOTES

1. G. A. Mourou, C. P. J. Barty, and M. D. Perry, "Ultrahigh-intensity lasers: physics of the extreme on a tabletop," Phys. Today **51**(1), 22–28 (1998).
2. R. W. Schoenlein, W. P. Leemans, A. H. Chin, P. Volfbeyn, T. E. Glover, P. Balling, M. Zolotorev, K. J. Kim, S. Chattopadhyay, and C. V. Shank, "Femtosecond x-ray pulses at 0.4 Å generated by 90° Thomson scattering: a tool for probing the structural dynamics of materials," Science **274**, 236–238 (1996).
3. H. Ihee, V. A. Lobastov, U. M. Gomez, B. M. Goodson, R. Srinivasan, C.-Y. Ruan, and A. H. Zewail, "Direct imaging of transient molecular structures with ultrafast diffraction," Science **291**, 458–462 (2001).
4. P. G. O'Shea and H. P. Freund, "Free-electron lasers: status and applications," Science **292**, 1855–1858 (2001).
5. D. Umstadter, "Review of physics and applications of relativistic plasmas driven by ultraintense lasers," Phys. Plasmas **8**, 1774–1785 (2001), and references therein.
6. T. Tajima and J. M. Dawson, "Laser electron accelerator," Phys. Rev. Lett. **43**, 267–270 (1979).
7. D. W. Forslund, J. M. Kindel, W. B. Mori, C. Joshi, and J. M. Dawson, "Two-dimensional simulations of single-frequency

and beat-wave laser-plasma heating," Phys. Rev. Lett. **54**, 558–561 (1985).
8. P. Sprangle, E. Esarey, A. Ting, and G. Joyce, "Laser wakefield acceleration and relativistic optical guiding," Appl. Phys. Lett. **53**, 2146–2148 (1988).
9. C. I. Moore, J. P. Knauer, and D. D. Meyerhofer, "Observation of the transition from Thomson to Compton scattering in multiphoton interactions with low-energy electrons," Phys. Rev. Lett. **74**, 2439–2442 (1995).
10. G. Malka and J. L. Miquel, "Experimental confirmation of ponderomotive-force electrons produced by an ultrarelativistic laser pulse on a solid target," Phys. Rev. Lett. **77**, 75–78 (1996).
11. G. Malka, E. Lefebvre, and J. L. Miquel, "Experimental observation of electrons accelerated in vacuum to relativistic energies by a high-intensity laser," Phys. Rev. Lett. **78**, 3314–3317 (1997).
12. C. I. Moore, A. Ting, K. Krushelnick, E. Esarey, R. F. Hubbard, B. Hafizi, H. R. Burris, C. Manka, and P. Sprangle, "Electron trapping in self-modulated laser wakefields by Raman backscatter," Phys. Rev. Lett. **79**, 3909–3912 (1997).
13. K.-C. Tzeng, W. B. Mori, and T. Katsouleas, "Electron beam characteristics from laser-driven wave breaking," Phys. Rev. Lett. **79**, 5258–5261 (1997).
14. C. Gahn, G. D. Tsakiris, A. Pukhov, J. Meyer-ter-Vehn, G. Pretzler, P. Thirolf, D. Habs, and K. J. Witte, "Multi-MeV electron beam generation by direct laser acceleration in high-density plasma channels," Phys. Rev. Lett. **83**, 4772–4775 (1999).
15. A. Pukhov, Z.-M. Sheng, and J. Meyer-ter-vehn, "Particle acceleration in relativistic laser channels," Phys. Plasmas **6**, 2847–2854 (1999).
16. W. Yu, V. Bychenkov, Y. Sentoku, M. Y. Yu, Z. M. Sheng, and K. Mima, "Electron acceleration by a short relativistic laser pulse at the front of solid target," Phys. Rev. Lett. **85**, 570–573 (2000).
17. X. Wang, M. Krishnan, N. Saleh, H. Wang, and D. Umstadter, "Electron acceleration and the propagation of ultrashort high-intensity laser pulses in plasmas," Phys. Rev. Lett. **84**, 5324–5327 (2000).
18. V. Malka, J. Fauer, J. R. Marquès, F. Amiranoff, J. P. Rousseau, S. Ranc, J. P. Chambaret, Z. Najmudin, B. Walton, P. Mora, and A. Solodov, "Characteristics of electron beams produced by ultrashort (30 fs) laser pulses," Phys. Plasmas **8**, 2605–2608 (2001).
19. D. Giulietii, M. Galimberti, A. Giulietti, L. A. Gizzi, M. Borghesi, Ph. Balcou, A. Rousse, and J. Ph. Rousseau, "High-energy electron beam production by femtosecond laser interactions with exploding-foil plasmas," Phys. Rev. E **64**, 015402-1–015402-4 (2001).
20. X. Wang, S. Backus, H. Kapteyn, M. Murnane, N. Saleh, D. Umstadter, and W. Yu, "Generation of megaelectronvolt electron beams by an ultrashort (<30 fs), intense laser pulse," in *Applications of High Field and Short Wavelength Sources*, Vol. 65 of OSA Trends in Optics and Photonics Series (Optical Society of America, Washington, D.C., 2001).
21. H. Wang, S. Backus, Z. Chang, R. Wagner, K. Kim, X. Wang, D. Umstadter, T. Lei, M. Murnane, and H. Kapteyn, "Generation of 10-W average-power, 24-fs pulses from a Ti:sapphire amplifier system," J. Opt. Soc. Am. B **16**, 1790–1794 (1999).
22. The generated maximum electron density from the H_2 was $\sim 2.5 \times 10^{19}$ cm^{-3}, one fifth of that from the N_2 under the same backing pressure. For the laser conditions described in the text, no MeV electrons were observed with H_2 or at such densities.
23. S. Augst, D. Strickland, D. D. Meyerhofer, S. L. Chin, and J. H. Eberly, "Tunneling ionization of noble gases in a high-intensity laser field," Phys. Rev. Lett. **63**, 2212–2215 (1989).
24. D. Umstadter, S.-Y. Chen, A. Maksimchuk, G. Mourou, and R. Wagner, "Nonlinear optics in relativistic plasmas and laser wake field acceleration of electrons," Science **273**, 472–475 (1996).
25. R. Wagner, S.-Y. Chen, A. Maksimchuk, and D. Umstadter, "Electron acceleration by a laser wakefield in a relativistically self-guided channel," Phys. Rev. Lett. **78**, 3125–3128 (1997).
26. A. Modena, Z. Najmudin, A. E. Dangor, C. E. Clayton, K. A. Marsh, C. Joshi, V. Malka, C. B. Darrow, C. Danson, D. Neely, and F. N. Walsh, "Electron acceleration from the breaking of relativistic plasma waves," Nature **377**, 606–608 (1995).
27. X. Wang, Q. Wang, and B. Shen, "Forward acceleration and the generation of femtosecond, magaelectronvolt electron beams by an ultrafast intense laser pulse," Chin. Opt. Lett. (to be published).
28. L. D. Landau and E. M. Lifshitz, *The Classical Theory of Fields*, 4th ed. (Butterworth-Heinemann, Oxford, 1979).
29. P. H. Bucksbaum, M. Bashkansky, and T. J. McIlrath, "Scattering of electrons by intense coherent light," Phys. Rev. Lett. **58**, 349–352 (1987).
30. A. Pukhov and J. Meyer-ter-Vehn, "Relativistic magnetic self-channeling of light in near-critical plasma: three-dimensional particle-in-cell simulation," Phys. Rev. Lett. **76**, 3975–3978 (1996).
31. J. C. Adam, A. Hèron, S. Guèrin, G. Laval, P. Mora, and B. Quesnel, "Anomalous absorption of very high-intensity laser pulses propagating through moderately dense plasma," Phys. Rev. Lett. **78**, 4765–4768 (1997).
32. E. Esarey and M. Pilloff, "Trapping and acceleration in nonlinear plasma waves," Phys. Plasmas **2**, 1432–1436 (1995).
33. S. Backus, C. G. Durfee III, G. Mourou, H. C. Kapteyn, and M. M. Murnane, "0.2-TW laser system at 1 kHz," Opt. Lett. **22**, 1256–1258 (1997).
34. O. Albert, H. Wang, D. Liu, Z. Chang, and G. Mourou, "Generation of relativistic intensity pulses at a kilohertz repetition rate," Opt. Lett. **25**, 1125–1127 (2000).